J. Phycol. **35,** 42–53 (1999)

PHOTOSYNTHESIS-IRRADIANCE PATTERNS IN BENTHIC MICROALGAE: VARIATIONS AS A FUNCTION OF ASSEMBLAGE THICKNESS AND COMMUNITY STRUCTURE

Walter K. Dodds,[2] *Barry J. F. Biggs, and Rex L. Lowe*[3]

National Institute of Water and Atmospheric Research Ltd., P.O. Box 8602, Christchurch, New Zealand

Photosynthesis-irradiance (P-I) characteristics of periphyton (microphytobenthos) have been considered primarily for entire assemblages. How P-I responses vary with mat thickness and with community composition has not been considered in detail. We used a combined approach of modeling, microscale determinations of photosynthetic rate and light attenuation, and whole-assemblage O_2 flux measurements to explore P-I relationships. The modeling approach suggested that the onset of photosynthetic saturation and photoinhibition will occur at higher irradiance and that whole-mat photoinhibition (decreased photosynthesis at very high irradiance), biomass-specific maximum photosynthetic rate, and initial slope of the P-I function (α) should decrease as assemblage thickness increases or light attenuation increases. Spherical light microsensor profiles for a variety of stream algae indicated a strongly compressed photic zone with attenuation coefficients of 70–1791 m^{-1} for scalar photosynthetic photon fluence density. The O_2 microelectrode measurements showed little if any photoinhibition at 2 and 4 mm depths in one filamentous green algal (*Ulothrix*) assemblage, with a relatively low attenuation coefficient, and no photoinhibition in a second *Ulothrix* community. An assemblage dominated by a unicellular cyanobacterium exhibited little photoinhibition at 2 and 4 mm, and a dense cyanobacterial (*Phormidium*)/xanthophyte (*Vaucheria*) community exhibited no photoinhibition at all. The microelectrode data revealed increases in α over several millimeters of depth (photoacclimation). These data supported the model predictions with regard to the effects of mat optical thickness on whole-assemblage values for α and photoinhibition. Whole-community O_2 flux data from 15 intact assemblages revealed positive relationships between chlorophyll *a* density and maximum photosynthetic rate or α expressed per unit area; the relationships with chlorophyll *a* were negative when photosynthetic rates were expressed per unit chlorophyll *a*. None of the whole assemblages exhibited photoinhibition. Thus, the data from the whole communities were consistent with model predictions.

Key index words: **biofilm; light; microphytobenthos; periphyton; photosynthesis-irradiance**

Abbreviations: **NPP, net primary production; P-I, photosynthesis-irradiance; P_{max}, maximum photosynthetic rate; PPFD, photosynthetic photon fluence density; R, respiration**

Periphyton assemblages (algal biofilms) can be responsible for the majority of production in shallow, unshaded, aquatic habitats. Clear and unshaded streams, shallow lakes, wetlands, and shallow coastal waters are all habitats where such production should be important. The effects of irradiance on periphyton photosynthetic rates have been characterized for only a few habitats (e.g. Hill 1996), despite the central role that benthic microalgae may play in clear shallow waters. In contrast, photosynthesis-irradiance (P-I) relationships have been documented for a wide variety of unialgal cultures, marine and freshwater phytoplankton assemblages, and terrestrial plants (Enríquez et al. 1996).

Photosynthesis-irradiance relationships have four main descriptive features: the maximum photosynthetic rate (P_{max}), the initial rate of increase of photosynthesis as light increases from darkness (α), the amount of photoinhibition (β), and respiration (R). Broad-scale comparisons of terrestrial plants, aquatic plants, and microalgae have shown that P_{max}, R, and α vary as a function of thickness of the photosynthetic assemblage. R, P_{max}, and α all are positively interrelated, and if they are expressed per unit carbon, all three decrease as thickness increases (Enríquez et al. 1996). However, these empirical comparisons did not include intact algal biofilms, where many species may cooccur, and did not provide explicit models that account for the differences with thickness.

In this paper, we refer to photoinhibition as a statistically significant decrease in photosynthetic rate (β) when irradiance increases past the point of maximal photosynthesis. More recently, it has been shown that some damage to photosystem II occurs even at low irradiance (Anderson et al. 1997), and photoinhibition occurs even though β is not significant. We will use β as an index of photoinhibition but revisit the newer concept of photoinhibition in the discussion.

The discrepancy between the way photoinhibition is viewed in periphyton and in other photosynthetic communities provides one example of how periphy-

[1] Received 18 March 1998. Accepted 16 October 1998.

[2] Present address and author for reprint requests: Division of Biology, Kansas State University, Manhattan, Kansas 66506; e-mail wkdodds@ksu.edu.

[3] Present address: Department of Biological Sciences, Bowling Green State University, Bowling Green, Ohio 43403.

TABLE 1. Parameters used to provide values for the model.

Parameter	Range (units)	System (reference)
η (light attenuation)	1203–3108 (m^{-1})	*Ulothrix* and diatom communities (Dodds 1992)
η	70–1790	Eight periphyton communities (this study)
η	4540	Dense cyanobacterial film (Kühl et al. 1996)
P_{max} (maximum photosynthesis)	7–20 (mg C·g C^{-1}·h^{-1})	25%–75% quartiles, 62 microalgal studies (Enríquez et al. 1996)
α (initial slope)	0.1–3 (mg C·g C^{-1}·h^{-1}[μmol photon·m^{-2}·h^{-1}]$^{-1}$)	95% confidence intervals, 62 microalgal studies (Enríquez et al. 1996)
β (inhibition constant)	0–0.1 (mg C·g C^{-1}·h^{-1}[μmol photon·m^{-2}·h^{-1}]$^{-1}$)	Platt et al. 1980
g chl *a*/g carbon	0.07	Mean 62 microalgal studies (Enríquez et al. 1996)

ton could potentially differ from other more studied systems. Photoinhibition can lower production of terrestrial plants and marine phytoplankton (Long et al. 1994). In contrast, Hill (1996) speculated that photoinhibition of periphyton can occur only when shade-acclimated communities are exposed to full sunlight. Thus, the existence of photoinhibition and its importance to periphyton are somewhat controversial. This may be because models are not available that elucidate conditions under which photoinhibition may occur under natural conditions in periphyton. Pinpointing mechanisms may not be a purely physiological exercise; an understanding of photoinhibitory processes in periphyton may be important in explaining the influence of increased UV irradiance on primary production and the interplay between primary producers and consumers (e.g. Bothwell et al. 1994).

The tools to assess physiological parameters of periphyton assemblages at scales relevant to the individual organisms in these communities are now available. Microscale O_2 probes can measure photosynthetic rate with as little as 100 μm spatial resolution (e.g. Revsbech and Jørgensen 1983). The ambient light field is attenuated considerably within 1 mm in benthic microalgal assemblages (Jørgensen and DesMarais 1988, Dodds 1989a). The O_2 microelectrodes can be combined with scalar light microsensors (Dodds 1992, Lassen et al. 1992) to generate P-I curves within the compressed photic zones common in lighted benthos (Dodds 1992, Kühl et al. 1996). Despite the wide variety of periphyton communities found in aquatic habitats, comparatively few have been analyzed in such fashion.

The objective of this study was to describe how P-I characteristics of entire periphyton assemblages vary as functions of mat thickness (biomass) and community type. A model was constructed that explicitly addresses effects of increased thickness and variation of light attenuation coefficients. Our measurements of microscale P-I responses and light attenuation of periphyton communities and previously published data provided parameters for the model. Our microscale and macroscale measurements provided a basis for testing model predictions.

MATERIALS AND METHODS

Model. Photosynthetic rate is calculated at each depth within the algal biofilm as a function of surface irradiance, light attenuation, and P-I characteristics. The P-I characteristics are modeled and described with the equations of Platt et al. (1980). The central equation is

$$P = P_s(1 - e^{-\alpha I/P_s})e^{-\beta I/P_s} \quad (1)$$

where P = photosynthetic rate, P_s = maximum photosynthesis in the absence of photoinhibition under optimal light, α = the slope of the line at low light, β = the photoinhibition constant, and I = irradiance. Derived parameters were described by Platt et al. (1980): P_{max} is the maximum observed photosynthetic rate, I_m is the irradiance where P_{max} occurs, I_k is the irradiance where the onset of saturation of photosynthetic rate occurs (P_{max}/α), and I_b is the irradiance where the onset of photoinhibition occurs.

In the model, gross primary production is calculated as biomass carbon-specific photosynthetic rate at 100 μm intervals down through the mat. The rate at each depth depends on light levels calculated from a model of light attenuation with depth (see below). Initial surface light intensities varied from 0 to 2000 μmol quanta·m^{-2}·s^{-1} in 20 increments. The averaged model output for each thickness at each irradiance then was used to determine a biomass-specific P-I curve for the entire assemblage with nonlinear curve fitting using a quasi-Newton method for parameter estimation. When photoinhibition was not evident for the entire assemblage (no decrease in photosynthetic rate at high irradiance, or equation 1 fit the model output with a negative value for β), the Jassby and Platt (1976) equation was used to fit the model output.

$$P = P_{max}\tanh\left(\frac{\alpha I}{P_{max}}\right) \quad (2)$$

The input values for the model were taken from literature values for P_s, α, and β (Table 1). Values for P-I relationships were taken from phytoplankton measurements because they are measured across a shallow light gradient (i.e. a typical field or laboratory bottle experiment with phytoplankton does not contain a significant light gradient within the bottle, whereas the typical whole-assemblage periphyton experiment is done with an assemblage that has a steep light gradient within it). Because we modeled individual depths of 100 μm thickness, the shallow light gradient in bottle experiments should approximate that in each 100-μm thick layer. Biomass in the model is presented as carbon, and photosynthetic assimilation is scaled by mass of carbon in the model. Irradiance (I) is presented as μmol photons·m^{-2}·s^{-1} photosynthetic photon fluence density (PPFD).

Biomass and light attenuation are modeled as constant through the entire assemblage. Ramifications of these assumptions will be covered in the Discussion. An attenuation coefficient was used to calculate the light transmitted through each layer. The maximum light at the surface was assumed to be 2000 μmol quanta·m^{-2}·s^{-1}, because this is close to the maximum PPFD found naturally in shallow surface waters. The light at each depth was calculated using the equation

TABLE 2. Characteristics of periphyton communities used for light attenuation (η) and microelectrode experiments. Number of samples (N) and standard deviation (SD) for determination of η.

Date	Community dominants	Common or abundant	Chl *a* ($mg \cdot m^{-2}$)	Chl *a* ($mg \cdot cm^{-3}$)	η (m^{-1})	SD	N
24 Jan.	*Ulothrix*	*Synedra ulna* *Cymbella kappii*	250	0.124	72.4	1072.9	16
24 Jan.	unicellular cyanobacterium	*Cymbella kappii*	8552	11.11	589.4	430.9	15
24 Jan.	*Cymbella kappii*	*Ulothrix, Spirogyra, Synedra ulna, Fragilaria*	289	0.288	213.5	269.4	16
24 Jan.	*Batrachospermum*	*Synedra ulna*	806	0.402	71.8	128.9	16
24 Jan.	detritus and diverse assemblage including all diatoms and unicellular cyanobacterium above	diverse diatoms	4223	2.111	284.9	197.7	16
24 Jan.	low-light moss and *Microspora*	*Cocconeis, Synedra ulna, Fragilaria*	174	0.0807	230.0	210.3	16
24 Jan.	*Oedogonium*	*Ulothrix, Spirogyra, Synedra ulna, Fragilaria*	322	0.322	393.1	447.0	16
14 Feb.	*Ulothrix*	*Synedra ulna, Cymbella kappii*	694	1.387	36.2	35.5	15
16 Feb.	*Ulothrix*	*Fragilaria*	694	1.387	195.7	80.0	2
20 Feb.	unicellular cyanobacterium	*Cymbella kappii*			378.6	260.8	6
1 Mar.	*Phormidium*	*Vaucheria*	1988	1.988	1791	1242	8
6 Apr.	*Ulothrix*	*Fragilaria, Synedra ulna*	1600	3.200	209.1	70.8	6

$$I_2 = I_1 e^{(-\eta z)} \quad (3)$$

where I_1 and I_2 are irradiances at depths 1 and 2, respectively; z is the distance between depths 1 and 2 in meters; and η is the attenuation coefficient. We used light microprobes to establish additional coefficients for a variety of assemblages given the limited range of attenuation coefficients available in the literature (Table 1).

Microscale measurements. Irradiance was measured with a 200-μm diameter spherical light microprobe constructed with epoxy doped with titanium dioxide. Light was transmitted down the axis of the fiber from the end away from the spherical tip during construction (Lassen et al. 1992) to allow fabrication to within 10% of anisotropic response. The light collected during measurements by the probe passed through a 400–700-nm cutoff filter before the photodiode to exclude all but PPFD, and a silicon photodiode with an integral amplifier was used to assess irradiance (Dodds 1992). The absolute response of the probe was calibrated against the output of a LI-COR PAR (PPFD) sensor against a directional light source. The signal from the photodiode was averaged over a 5-s period with a LI-COR 1000 data logger to compensate for short-term fluctuation in light induced by movement of the water surface and undulation of filamentous algal masses.

Attenuation coefficients for a variety of benthic algal assemblages were estimated to provide a range of values for use in the model. A halogen fiber-optic light source, operated at 530 μmol photons$\cdot m^{-2} \cdot s^{-1}$, was placed directly above the assemblage, and the microprobe was placed with the axis of the fiber at 45° from vertical. Thus, the micromanipulator holding the fiber was moved forward 2 mm for each 1 mm increase in depth. Four separate profiles of each of seven assemblages were measured and additional profiles were generated from communities used for microscale photosynthetic rate measurements. All of these assemblages were collected from the Kaiapoi River at the NIWA Silverstream Research Facility (20 km north of Christchurch, New Zealand) on 24 January 1997 (Table 2). All except the moss with green algal filaments were collected from unshaded habitats, and light profiles were measured within 15 min of collection. Equation 3 was used to calculate attenuation from each depth to the next within each profile.

Gross photosynthetic rate was measured with O_2 microelectrodes in four communities (collected and analyzed on 16 and 20 February, 1 March, and 6 April 1997, Table 2) at each of three depths in the mat (0, 2, and 4 mm) to test the predictions of the model. The use of O_2 microelectrodes to determine gross photosynthetic rates was described by Revsbech and Jørgensen (1983), Glud et al. (1992), and Kühl et al. (1996). A cathode-type electrode with a 20-μm diameter tip encased in a stainless hypodermic needle was used. Sensors larger than 5 μm are more sensitive to water velocity and the O_2 microelectrode method for measuring photosynthesis does not work in flowing water. For these reasons, all algal assemblages were collected from slowly moving water (<0.05 m$\cdot s^{-1}$ at 2 mm from the assemblage surface, as measured with a thermistor microsensor (LaBarbera and Vogel 1976)), and all small-scale photosynthetic measurements were made in still water. If O_2 became greater than 50% above saturation, the water was circulated in the measurement chamber to avoid excessive supersaturation. The O_2 sensor in the needle minimized breakage of the probe during measurements. Disruption of the communities by the needle was minimal in all but one of the four communities studied (*Phormidum/Vaucheria*).

A sample of unicellular cyanobacteria (20 February 1997) was collected from the bottom of a slow-moving channel with a syringe and allowed to settle in the measurement vessel for 15 min before microscale measurements of photosynthetic rate were made. The remaining communities were removed carefully from the water so they remained intact and were analyzed immediately after collection. The epilithic samples remained attached to substrata during measurement. The samples were immersed in stream water at ambient temperatures during measurements. All measurements for each sample were made within 2 h, and the maximum temperature rise during the measurements was 1.5° C.

Illumination was provided by a fiber-optic halogen light source to minimize sample heating and allow for constant illumination. The O_2 microsensor was positioned at the surface of the assemblage, the light probe was positioned about 2 mm adjacent to the probe at the surface, the fiber-optic light source was turned on, and O_2 was allowed to come to equilibrium. The light was turned off, and the rate of decrease in O_2 concentration over the first 5 s after darkening was used to estimate gross photosynthetic rate. This length of time results in a maximum spatial resolution of 150 μm (see calculations in Revsbech & Jørgensen 1983). Our measurements were made every 2 mm. The light was turned on again, the probe was moved down to the next depth, and the photosynthesis measurement was repeated. The intensity of the light was altered after measurements were made at each depth by changing the distance of the terminating end of the illumination source from the sample. Measurements were made in short groups of three or four profiles under decreasing or increasing irradiance between measurements. This cycling from low to high irradiance and back again was used to avoid vertical redistribution of phototactic motile cells during the measurements. Surface irradiance was recorded with the light microprobe at the time of each measurement. After all the photosynthetic rate measurements were made, the fiber-optic light sensor was placed at 2 mm and then at 4 mm in the mat at the position where those measurements were made to estimate the proportion of surface light that reached each depth. These light attenuation measurements were done in triplicate in the region of photosynthesis measure-

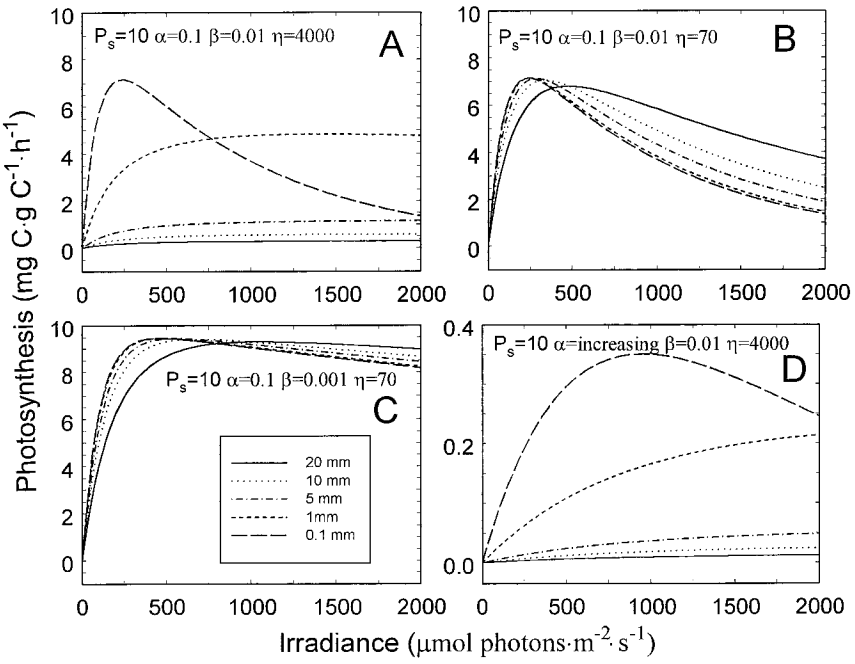

FIG. 1. Results from the photosynthesis- irradiance models of periphyton assemblages of different thickness with high attenuation/high photoinhibition (A), low attenuation (B), low attenuation/low photoinhibition (C), and increasing α (D). To compare total photosynthesis, multiply by depth. See Table 3 for the parameters that characterize these curves.

ments. The resulting P-I curves were fit to equation 1 or 2 as described for analysis of the model output.

Macroscale measurements. Fifteen sets of P-I experiments were performed on natural whole-rock communities in a sealed Plexiglas chamber with recirculating water (internal dimensions of the chamber were 0.16 m deep by 0.38 m long by 0.19 m deep, 14 L total volume). The chamber was submerged in a 0.3-m deep run of the Kakanui River, South Island of New Zealand, to maintain ambient temperature. Water was pumped through the closed system using a submersible pump in the return hose. Velocities in the chamber were 0.2–0.3 m·s^{-1} based on the cross-sectional area of the chamber and pump discharge (measured previously with an in-line flow meter, Biggs and Hickey 1994).

For each metabolic experiment, whole rocks that had been exposed to natural light regimes in clear waters were collected from areas of negligible riparian shading with velocities similar to those generated within the chamber. Up to eight rocks that appeared to have similar biomass and community composition were used for each experiment. Four experiments were performed with a low biomass community dominated by *Gomphoneis minuta* var. *cassieae* (diatom) to assess P-I relationships in thin-film communities and potential variability in these relationships, then all other experiments were done in duplicate. These included moderate and high biomass, *Gomphoneis*-dominated communities; a *Brachysira*-dominated diatom community; a *Cymbella/Gomphonema*-dominated diatom community; a *Spirogyra* (filamentous green algae) community; and a *Phormidium*-sp.-dominated cyanobacterial mat. One replicate from the *Cymbella/Gomphonema* community was rejected because of problems with drift in the O_2 measurements.

Dissolved O_2 was monitored using a YSI-DO probe (Yellow Springs Instruments, Yellow Spring, OH) inserted in the flow line and a scaling amplifier to subtract the background O_2 concentration and amplify the working range (usually 1 mg·L^{-1}) to full range on a chart recorder. Measurements of O_2 change were made over 3- to 5-min periods for each of 6–8 light treatments to calculate irradiance-specific net primary production (NPP) from linear sections of the recordings. At least 1.5 min equilibration time was allowed before each successive treatment effect was recorded. Light was attenuated in decreasing steps with successive layers of shade cloth and a final opaque rubber sheet (dark to determine community respiration). Light was monitored throughout each experiment using a submersible cosine LICOR PAR (PPFD) sensor. Gross primary production was determined as the sum of NPP and respiration. Photosynthesis-irradiance curves were fit to net photosynthetic rates for each community using the hyperbolic tangent model without photoinhibition (equation 2), with an additional term for community respiration (R).

At the completion of each experiment, the volume of water in the chamber was measured, then the entire surface area of each rock in the chamber was scrubbed free of periphyton in 2 L of river water as described by Biggs and Close (1989). This sample was returned to the laboratory and frozen at −20° C until analysis. Dimensions of the rocks were measured and used to determine surface area, employing the equation of Biggs and Close (1989). Ambient stream temperatures during these experiments were 15°–19° C. Temperatures within the chamber did not increase by more than 2° C during any experiment.

In the laboratory, each periphyton sample was thawed and homogenized using a blender (Biggs 1987). The sample was then transferred into a narrow-necked bottle, brought to a known volume, and shaken thoroughly to obtain a suspension from which a subsample was withdrawn. The total density of cells and relative abundance of common taxa were then assessed under 400× magnification. Three, 5-mL aliquots per sample were removed from the suspension (after shaking between each aliquot) and pooled. This was repeated five times for each sample to give five analytical replicates. These were filtered to concentrate the periphyton for spectrophotometric analysis of chlorophyll *a* (chl *a*) using boiling 90% ethanol as extractant, correcting for phaeopigments by acidification, and employing a chl *a* absorption coefficient of 28.66 cm^{-1} (Sartory and Grobbelaar 1984). The subsampling and filtering procedure was repeated for determination of ash-free dry mass (AFDM) by drying at 105° C for 24 h and ashing at 450° C for 4 h.

RESULTS

Model predictions. The model indicated that the general effects of increasing assemblage thickness or light attenuation coefficients should decrease in α, β, and P_{max} when expressed per unit biomass. Increases in I_m, I_k, and I_b with greater thickness were also predicted (Fig. 1, Table 3). These simulations suggest that photoinhibition of relatively thick (e.g. >5 mm) periphyton assemblages is unlikely unless

TABLE 3. P-I parameters for the four sets of curves in Figure 1. Empty cells in a row indicate that the hyperbolic tangent function, without photoinhibition, gave the best fit to the data. See Table 1 for units on parameters. Conditions for each run are set by light attenuation and values for α, P_s, and β at 0.1 m depth, except for the last run, where α was initially set to 0.001 then increased by 3% every 0.1 mm.

Light attenuation	Thickness (mm)	α	P_s	β	P_{max}	I_m	I_k	I_b
4000	0.1	0.100	10.00	0.0100	7.15	104	72	1000
4000	1.0	0.097	10.00	0.0097	7.15	108	74	1036
4000	5.0	0.084	9.99	0.0083	7.17	124	85	1206
4000	10.0	0.071	9.77	0.0067	7.07	147	100	1455
4000	20.0	0.051	9.09	0.0041	6.84	202	135	2243
70	0.1	0.100	10.00	0.0100	7.15	104	72	1000
70	1.0	0.017	—	—	4.76	—	285	—
70	5.0	0.003	—	—	1.12	—	333	—
70	10.0	0.002	—	—	0.57	—	333	—
70	20.0	0.001	—	—	0.28	—	324	—
70	0.1	0.100	10.00	0.0010	9.45	200	95	10,000
70	1.0	0.095	10.00	0.0010	9.45	210	99	10,342
70	5.0	0.084	9.99	0.0008	9.44	239	113	11,974
70	10.0	0.070	9.93	0.0007	9.41	286	134	14,803
70	20.0	0.038	—	—	9.16	—	243	—
4000	0.1	0.001	10	0.001	0.351	350	914	1000
4000	1.0	0.000229	—	—	0.2148	—	940	—
4000	5.0	0.000050	—	—	0.0485	—	900	—
4000	10.0	0.000025	—	—	0.0245	—	980	—
4000	20.0	0.000013	—	—	0.0122	—	938	—

the attenuation coefficient is low (see below). To determine total photosynthesis for areal rates, it is necessary to multiply biomass-specific photosynthetic rate (e.g. data in Fig. 1) by the biomass of the layer and sum all of the layers. When this approach is used, photosynthetic rate of the assemblage increases as thickness becomes greater, up to a point. When attenuation coefficients are high, the lowermost layers receive little light and make only a small contribution to total photosynthesis.

Light and photosynthetic microprofiles. The irradiance attenuation coefficients of the communities sampled ranged from 71 to 1791 m^{-1} with the steepest profiles in the unicellular cyanobacterium (Table 2, Fig. 2). The coefficients varied significantly ($P < 0.028$, $F = 2.507$, ANOVA) among the communities, but not when analyzed by depth or by individual profile. This suggests that taxonomic composition is a more important determinant of light attenuation in periphyton communities than variation with depth or where a profile is measured (horizontal position) in each type of mat. The data suggest that the assumption of constant attenuation with depth in the model is realistic. The lack of significant increases in attenuation with depth suggests that deeper portions of the communities do not acclimate to lower light by increasing photosynthetic pigment concentrations overall. However, this observation should be viewed with caution, because the data were variable, the ANOVA may be subject to problems of spatial autocorrelation, and the light probes detected only PPFD and not specific wavelengths absorbed by algal pigments.

Microelectrode data on O_2 production supported the model prediction that photoinhibition should be rare or absent at greater depths, leading to whole assemblages that are not photoinhibited (Figs. 3–6, Table 4). In the first *Ulothrix* community (Fig. 3), only small values of β occurred at all depths and for the combined areal data. When light attenuation was moderate (cyanobacterial unicells), photoinhibition was mild at the surface but not important when the assemblage as a whole was considered (Fig. 4). In the community with the highest attenuation analyzed (*Phormidium/Vaucheria*), a curve could not be fit with a positive value for photoinhibition at any depth, and at 4 mm (Fig. 5B), no saturation was apparent (i.e. even the hyperbolic tangent model failed, and a linear model provided the best fit). In the filamentous *Ulothrix* community (6 April), neither photoinhibition nor saturation occurred (Fig. 6), even though this community had only moderate light attenuation relative to the other communities (Table 2).

The unicellular cyanobacterium-dominated community most closely matches the model assumptions of constant α with depth, because mixing the assemblage was necessary during collection. Thus, a consistent trend in I_k, I_b, or I_m with depth would not be expected. Biomass was apparently somewhat lower at 2 mm given the lower value of P_{max}. As predicted by the model, the areal value for I_k was above the average for the assemblage, and photoinhibition of areal photosynthesis was not evident.

Two of the remaining three communities (those that remained intact before analysis) showed a consistent increase in α with depth (Table 4). In the first *Ulothrix* assemblage, with relatively high light

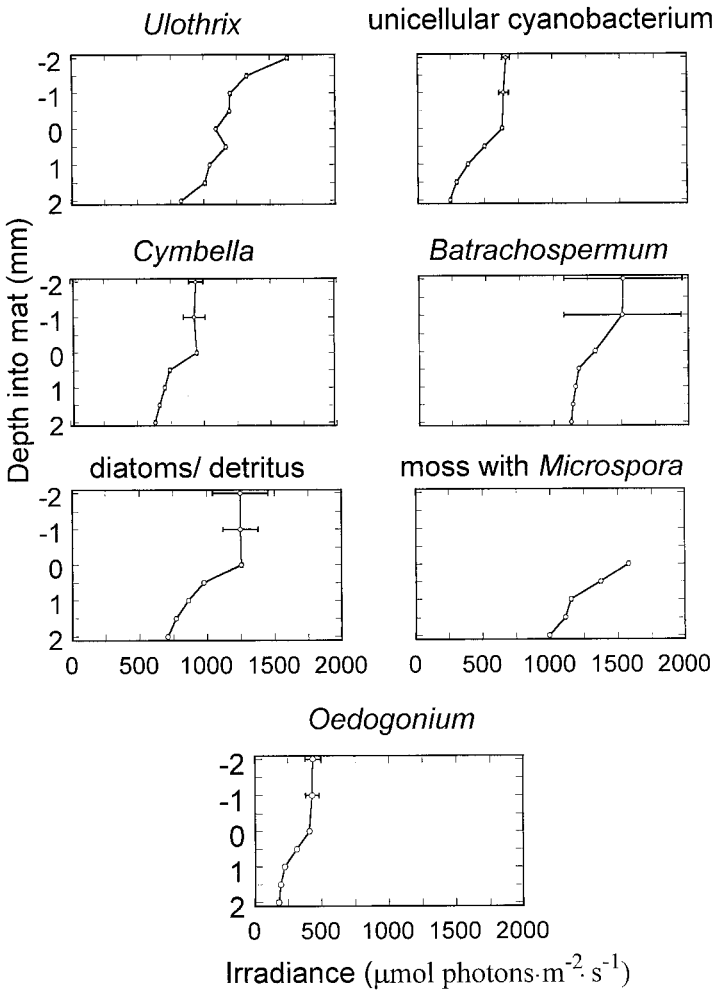

FIG. 2. Light attenuation profiles for five stream periphyton assemblages. Attenuation coefficients and community composition are listed in Table 2.

transmission, α increased by 50% over 4 mm (P = 0.035, regression of log-transformed α vs. depth). In the *Phormidium/Vaucheria* community, about a 30-fold increase in α occurred from the surface to 4 mm (P = 0.0074, regression of log-transformed α vs. depth). In the *Phormidium/Vaucheria* community, this led to a decrease in I_k with depth; in the *Ulothrix* community, I_k was lower at 2 and 4 mm than at the surface. No consistent trends occurred in P_{max} or β with depth. The 6 April sample of the *Ulothrix* com-

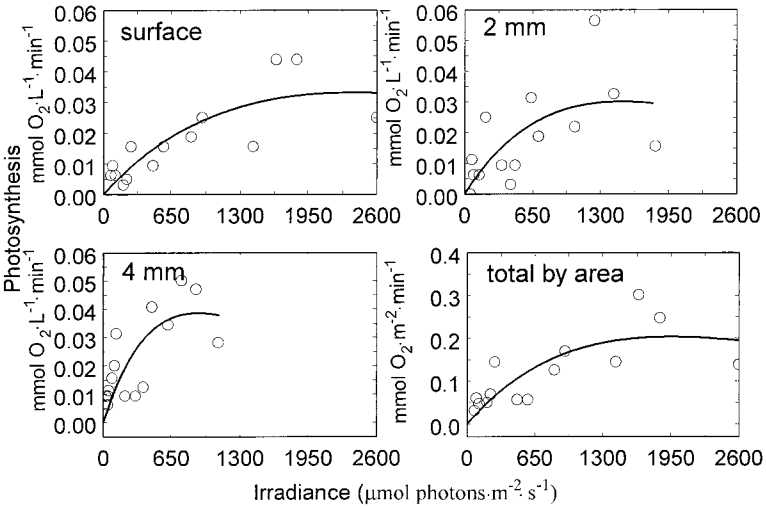

FIG. 3. Photosynthesis-irradiance characteristics at three distinct depths in a *Ulothrix* community (16 February 1997) expressed as a rate at each depth and as the computed rate of gross photosynthesis for total area.

TABLE 4. Parameters for the P-I curves for the communities given in Figures 2–4. Empty cells in a row indicate that the hyperbolic tangent function, without photoinhibition, gave the best fit to the data. Units of α and β are mmol $O_2 \cdot L^{-1} \cdot min^{-1}$ (μmol photon$\cdot m^{-2} \cdot s^{-1})^{-1}$ for specific depth and mmol $O_2 \cdot m^{-2} \cdot min^{-1}$ (μmol photon$\cdot m^{-2} \cdot s^{-1})^{-1}$ for areal rates. Units of P_{max} and P_s are mmol $O_2 \cdot m^{-1} \cdot min^{-1}$ for specific depth and mmol $O_2 \cdot m^{-2} \cdot min^{-1}$ for areal rates. At 4 mm in the *Phormidium/Vaucheria* community and at all depths in the 6 April *Ulothrix* community, a linear relationship fit the data, so only the slope (α) is reported.

Community	Depth (mm)	α	P_s	β	P_{max}	I_m	I_k (μmol photon$\cdot m^{-2} \cdot s^{-1}$)	I_b
Ulothrix (16 Feb. 1997)	0	0.00004	10.66	0.00445	0.0332	1036	878	2396
	2	0.00005	111.35	0.06350	0.0303	761	645	1754
	4	0.00006	110.01	0.05890	0.0386	811	687	1868
	areal	0.00028	108.90	0.05547	0.2032	850	720	1963
Cyanobacterial unicells (20 Feb. 1997)	0	0.00023	23.55	0.02410	0.0810	422	358	977
	2	0.00014	16.10	0.04450	0.0190	157	133	362
	4	0.00045	13.52	0.02226	0.1006	261	221	680
	areal	0.00092	—	—	0.3214	—	350	—
Phormidium/Vaucheria (1 Mar. 1997)	0	0.00039	—	—	0.1502	—	385	—
	2	0.00220	—	—	0.2927	—	133	—
	4	0.01164	—	—	—	—	—	—
	areal	0.00220	—	—	1.1199	—	508	—
Ulothrix (6 Apr. 1997)	0	0.00115	—	—	—	—	—	—
	2	0.00141	—	—	—	—	—	—
	4	0.00239	—	—	—	—	—	—
	areal	0.00600	—	—	—	—	—	—

munity had higher α at 2 and 4 mm, but this increase was not significant.

The microelectrode data suggested that a model with increased α with depth may represent at least some natural communities. Consequently, the model was rerun with α increasing by 1.03 per 0.1 mm (Fig. 1D, Table 3). The results of this simulation suggested that photoinhibition is even less likely if the periphyton assemblage has greater α with depth. However, with α increasing, the value for I_k showed no clear trend as depth increased.

Whole-community metabolism. The whole-community analyses included diatom-, green algae-, and cyanobacterial-dominated mats (Table 5). They varied in biomass by 19-, 12-, and 164-fold when expressed as chl *a,* AFDM, and cell volume per unit area, respectively (Table 5). In all cases, the hyperbolic tangent P-I function (equation 2) fit the photosynthetic data well ($r^2 > 0.95$). No strong evidence for photoinhibition was seen in any of the assemblages, including the filamentous algal assemblage (*Spirogyra*), which potentially had relatively low light attenuation.

High variability (6.5–12.2-fold) occurred in α, R, I_k, and I_c (the irradiance at which compensation occurs [i.e. gross photosynthesis = respiration]) in the four replicates for the *Gomphoneis*-dominated diatom communities, which varied in chl *a* biomass by a factor of only 1.7 (coefficient of variation [CV] = 24%) (Table 5). Conversely, P_{max} was reasonably consistent among the replicates, varying by a factor of only up to 1.38 (CV = 14.7% and 14.0% for area and chlorophyll-specific P_{max}, respectively).

Pooled data showed significant positive correlations between algal biomass (chl *a*) and P_{max} and α

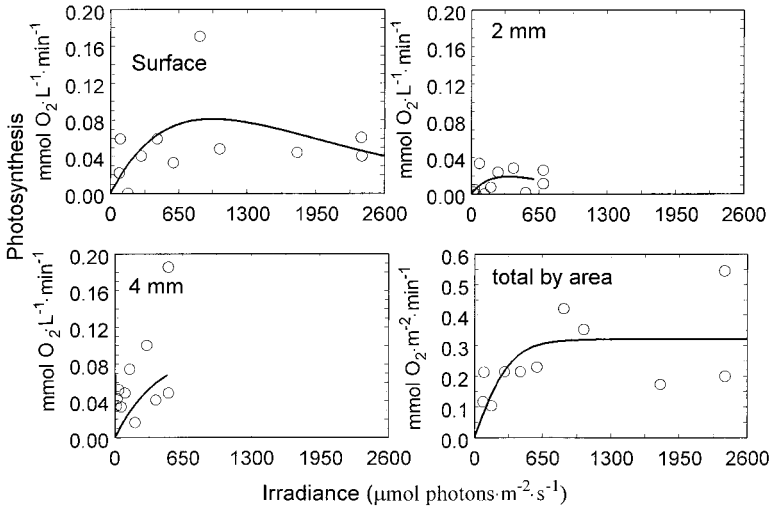

FIG. 4. Photosynthesis-irradiance characteristics at three distinct depths in a unicellular cyanobacterial community (20 February 1997) expressed as a rate at each depth and as the computed rate of gross photosynthesis for total area.

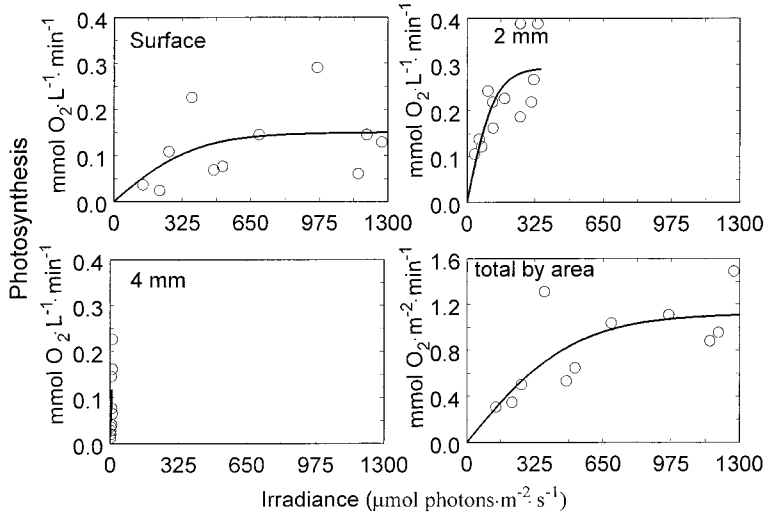

FIG. 5. Photosynthesis-irradiance characteristics at three distinct depths in a *Phormidum/Vaucheria* community (1 March 1997) expressed as a rate at each depth and as the computed rate of gross photosynthesis for total area.

when expressed per unit area (Fig. 7, Kendall's tau nonparametric correlation, $P = 0.0025$ and 0.0284, respectively). However, the correlations for both P_{max} and α were negative when expressed per unit biomass (Fig. 7, Kendall's tau nonparametric correlation $P = 0.037$ and 0.035, respectively). These data are consistent with predictions of the model.

The photosynthetic parameters did not vary with taxonomic composition. The *Cymbella/Gomphonema* community may have been different from the others (Fig. 7, Table 5). Unfortunately, the replicate for this community was lost because of probe signal drift, precluding statistical analysis.

No significant relationship occurred between I_k and thickness (chl *a*) in the 15 communities ($P > 0.05$, Kendall's tau correlation). This is what was predicted with model simulations when α increased with depth, but not when α was constant with depth.

DISCUSSION

Microscale patterns. Light attenuation values in this study are somewhat lower than those reported by others using optical fibers to characterize periphyton communities (Dodds 1992, Kühl et al. 1996). Those studies have focused on highly productive systems, such as an urban drainage ditch (Dodds 1992) or a cyanobacterial mat from a trickling filter (Kühl et al. 1996), whereas we sampled a number of loose, filamentous periphyton assemblages of types that are common in moderately productive streams. The highly attenuative communities studied previously, particularly the cyanobacterial mats, are likely to be among the most attenuative of all algal communities. Our results are useful because they indicate that a wider variation in light attenuation may occur in periphyton communities than had been described previously.

Scattering at the surface of some periphyton assemblages can increase light over the incident light by about 20% (e.g. Kühl et al. 1996). Analysis of data taken for light above six assemblages (Fig. 2) showed irradiance was not significantly greater at the surface than it was as the light probe moved away from the mat into the incident light field ($P >$

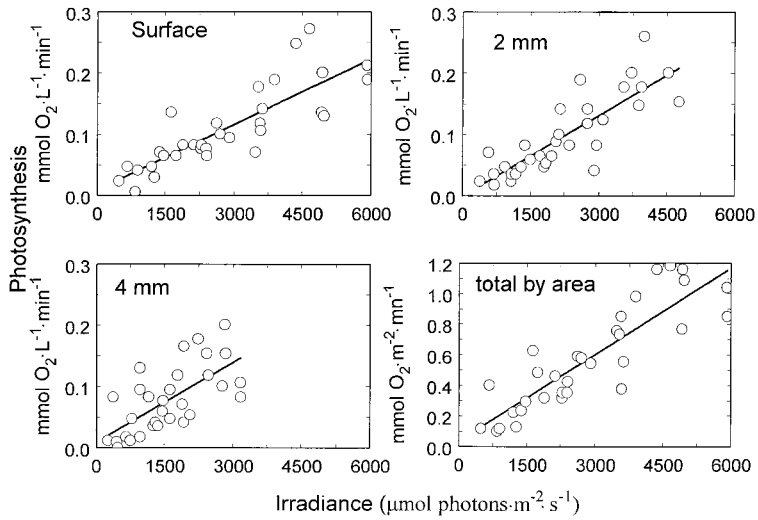

FIG. 6. Photosynthesis-irradiance characteristics at three distinct depths in a *Ulothrix* community (6 April 1997) expressed as a rate at each depth and as the computed rate of gross photosynthesis for total area.

TABLE 5. Photosynthesis-irradiance characteristics of 15 natural communities. P_{max} (area) and respiration (R) expressed as mg $O_2 \cdot m^{-2} \cdot h^{-1}$ and α (area) as mg $O_2 \cdot m^{-2} \cdot h^{-1} (\mu mol\ quanta \cdot m^{-2} \cdot s^{-1})^{-1}$. P_{max} (chl) expressed as mg $O_2 \cdot (mg\ chl\ a)^{-1} \cdot h^{-1}$ and α (chl) as mg $O_2 \cdot (mg\ chl)^{-1} \cdot h^{-1} (\mu mol\ photon \cdot m^{-2} \cdot s^{-1})^{-1}$. Units on R = mg $O_2 \cdot m^{-2} \cdot h^{-1}$ and I_k and I_c (compensation point) = μmol photon $\cdot m^{-2} \cdot s^{-1}$. The goodness of fit for nonlinear estimation by equation 2 is given in column r.

Community	Chl a ($mg \cdot m^{-2}$)	AFDM ($g \cdot m^{-2}$)	Cell volume ($\mu L \cdot m^{-2}$)	R	n	P_{max} (area)	α (area)	r	I_k	P_{max} (chl)	α (chl)	I_c
Gomphoneis 1a	11.5	7.12	7905	63	7	99.8	0.120	0.994	834	8.68	0.0104	620
Gomphoneis 1b	8.0	4.48	719	38	6	69.5	0.205	0.976	339	8.65	0.0255	208
Gomphoneis 1c	10.7	5.18	2486	41	7	87.0	0.341	0.997	255	8.17	0.0320	131
Gomphoneis 1d	14.6	7.44	934	46	7	91.9	0.982	0.976	94	6.31	0.0675	51
Gomphoneis 2a	50.3	17.81	38,131	160	8	427.1	0.938	0.992	455	8.50	0.0187	179
Gomphoneis 2b	41.8	28.56	22,167	121	7	220.7	1.172	0.978	188	5.28	0.0281	116
Gomphoneis 3a	63.7	35.47	57,821	284	7	443.8	0.968	0.992	458	6.97	0.0152	348
Gomphoneis 3b	64.5	44.21	20,620	162	7	254.6	1.400	0.968	182	3.94	0.0217	137
Brachysira a	10.8	5.77	2807	80	7	119.4	0.237	0.995	503	11.62	0.0219	408
Brachysira b	8.8	4.25	2696	65	9	87.3	0.409	0.970	214	9.93	0.0465	205

0.05, regression analysis). Thus, the increase in light at the surface from back-scattering is not a feature of all benthic algal assemblages, or increased illumination from back-scattering is only important at spatial scales smaller than 200 μm (the width of the probe).

Our model predictions and empirical measurements linking P-I relationships with assemblage thickness agree with the general trends noted by Enríquez et al. (1996). They noted a negative relationship between thickness and biomass-specific (per unit carbon) P_{max} and α. However, their analysis included microalgae only as single cells with a maximum thickness of 100 μm. The communities we analyzed were in the thickness ranges of macroalgae and terrestrial plant leaves; it is interesting that the mixed algal assemblages we studied yielded results similar to those for photosynthetic tissues of similar thickness (Enríquez et al. 1996). Our results also agree with the limited data already available for periphyton. Others have demonstrated that chlorophyll-specific α decreased as periphyton biomass accumulated (Hill and Boston 1991, Quinn et al. 1997), consistent with the broad taxonomic trends noted above and with our analysis.

The 15 whole communities did not exhibit decreased photosynthesis at the highest values of irradiance, which is consistent with data reviewed by Hill (1996). He suggested that whole periphyton communities should only show such decreases when they are acclimated to shade conditions then moved into full sun. Furthermore, Young and Huryn (1996) determined P-I relationships of gross primary production for a New Zealand river at eight sites over 2 years using whole-stream O_2 change methods. No photoinhibition was evident in their measurements, and 11 curves indicated no apparent saturation of production. Our analysis of small-scale

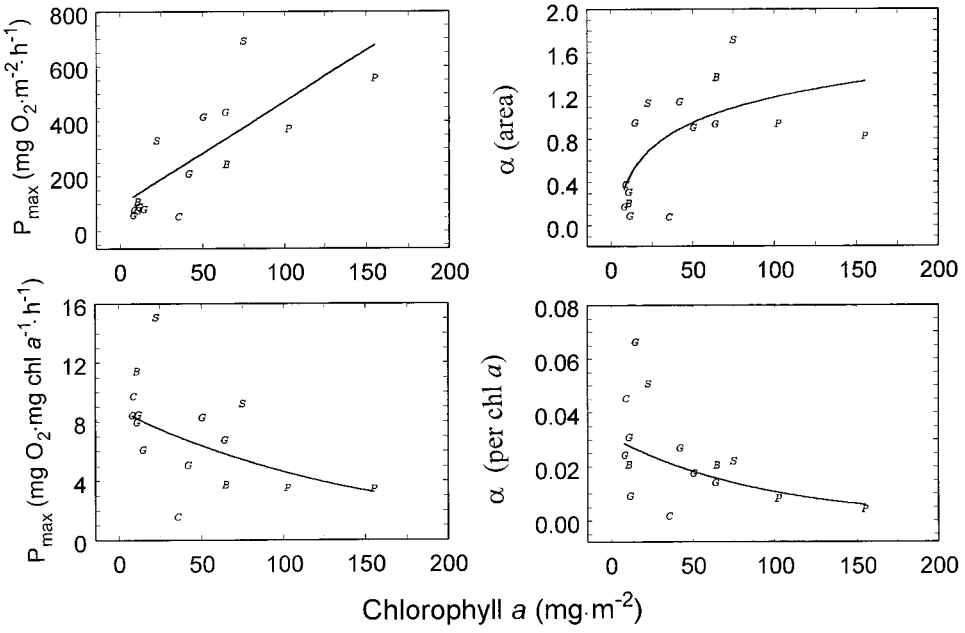

FIG. 7. Photosynthesis-irradiance parameters for whole communities from 15 separate sets of rocks with varied biomass or algal communities (*G, Gomphoneis minuta*-dominated communities; *C, Cymbella/Gomphonema*; *B, Brachysira*; *S, Spirogyra* spp.; *P, Phormidium* spp.) A linear relationship was used in the first panel and a second-order polynomial in the remaining three (R^2 areal P_{max} vs. chl a = 0.598; α vs. chl a = 0.775; chlorophyll-specific *Pmax* vs. chl a = 0.843; chlorophyll-specific α vs. chl a = 0.780). Parameters for each community are described in Table 5. Units for α (area) as mg $O_2 \cdot m^{-2} \cdot h^{-1} (\mu mol\ quanta \cdot m^{-2} \cdot s^{-1})^{-1}$ and α (chl) as mg $O_2 \cdot (mg\ chl)^{-1} \cdot h^{-1} (\mu mol\ photon \cdot m^{-2} \cdot s^{-1})^{-1}$.

P-I relationships suggests that even though photoinhibition may occur at the surface of periphyton mats, photoinhibition of whole communities should be rare because of the compensating influence of the deeper layers of the mat. Our simulations suggest that photoinhibition and even saturation is less likely if photoacclimation occurs with depth.

The increases in α would be more pronounced if our P-I data for microelectrodes were plotted as a function of just the wavelengths specifically available for photosynthesis. Our light attenuation values are for PPFD, and there are no spectral data for assemblages of the same genera as those we studied (but see Jørgensen and DesMarais 1988, Jørgensen et al. 1987 for data on other genera). The light quality in the assemblage likely changes with depth, with selective absorption of light by photosynthetic pigments. Thus, photoacclimation with depth may be even greater than our microelectrode data suggest.

In one set of microelectrode measurements, we did not observe saturation up to very high irradiance (Fig. 6) in a *Ulothrix* community. These results are similar to those from a *Ulothrix* community analyzed previously (Dodds 1992). A similar community collected and analyzed 6 weeks earlier (16 February) did exhibit saturation (Fig. 3). It had lower chlorophyll (by area and by volume) and lower light attenuation than the community that did not exhibit saturation. However, if the highest light point from each depth of the *Ulothrix* community from 16 February (Fig. 3) is omitted from the analysis, saturation becomes less pronounced. Other benthic cyanobacterial layers do not saturate up to 600 μmol photons·m^{-2}·s^{-1} (Lassen et al. 1997).

Previous studies also have demonstrated that photoacclimation can occur with depth in some periphyton assemblages (i.e. α increases with depth). A *Ulothrix* community exhibited increases in α over 1 mm depth, whereas a diatom assemblage did not over 0.5 mm depth (Dodds 1992). Two sandy marine sediment samples dominated by diatoms exhibited increases in α over the first several millimeters, followed by decreases with depth, and the third P-I profile in this marine study was characterized by a continuously decreasing α with depth (MacIntyre and Cullen 1995). Two profiles at 0.1 and 0.3 mm in a cyanobacterial mat showed decreased α values with increasing depth (Kühl et al. 1997).

The absolute photosynthetic rates obtained with microelectrodes should not be extrapolated to whole system rates for two reasons. First, the samples we analyzed were used because they were evidently taxonomically distinct and had high enough biomass to yield measurable photosynthetic rates. Thus, they were not intended to serve as assemblages representative of the entire system where they were collected. Second, measurements had to be made in still water. This may lead to slight depressions in P_{max} and more inhibition. However, the measurements still can be used for the purpose of our study, to investigate potential ranges in physiological properties as they vary among algal assemblages.

Macroscale patterns. We observed relatively high values for I_k in the whole communities. Of the 15 whole communities we studied, seven had I_k values above 400 μmol quanta·m^{-2}·s^{-1}, and the overall average was 391 μmol quanta·m^{-2}·s^{-1}; three of the four communities studied with microelectrodes had I_k values exceeding 400 μmol quanta·m^{-2}·s^{-1}. A wide range of values for I_k were obtained in eight previous periphyton studies reviewed by Hill (1996), but reported values fell between 20 and 400 μmol quanta·m^{-2}·s^{-1}, with most values between 200 and 400 μmol quanta·m^{-2}·s^{-1}. All of the communities we studied were collected in high-light habitats (austral summer, unshaded clear water streams), which may explain the relatively high values we observed for I_k.

Values of I_c were also relatively high for the 15 whole communities we studied with macroscale techniques. The mean value was 231 μmol quanta·m^{-2}·s^{-1}, which exceeded values recorded in all but one of six studies reviewed by Hill (1996). These generally high values for I_c suggest that many of the communities we studied were in a net heterotrophic state for much of the diurnal cycle. Net heterotrophic activity could be related to the respiratory demand of the algae and the heterotrophic organisms in the matrix. Our data on compensation points suggest that systems that appear autotrophic because they contain a high biomass of visible algae may not be so, particularly when light is reduced such as during cloudy days.

The data and simulation results in this paper suggest that photoinhibition (defined as a significant β) should be relatively rare in periphyton communities. Lack of photoinhibition previously has been attributed to compensation by deeper parts of the assemblage that masks it, an effect of measuring photosynthesis with UV-opaque incubation bottles and with light sources lacking in natural levels of UV and a consequence of short-term measurements of photosynthetic rate (Hill 1996). Similar mechanisms related to tissue thickness have been postulated to lead to lack of saturation of photosynthesis in shade-adapted fronds of *Laminaria* (Lüning 1979). Investigators using fluorescence techniques to investigate microphytobenthos also failed to observe photoinhibition (Kromkamp et al. 1998). Our microelectrode measurements were made with artificial light, and our whole-community measurements were made in UV-opaque plastic chambers, both over relatively short time periods. Nonetheless, we observed some evidence for weak photoinhibition at the surface of the assemblages in our microelectrode studies. Some studies previously have documented photoinhibition at the surface of epiphyte assemblages (Sand-Jensen and Revsbech 1987, Kühl et al. 1997). Longer incubations may be necessary to detect the damage associated with photoinhibition that occurs over minutes to hours (Long et al.

1994), but such incubations would be subject to problems such as sample heating, nutrient limitation, and other conditions not representative of natural habitats. The model and the microelectrode results do suggest that any photoinhibition at the surface of periphyton communities is likely to occur only within the top few millimeters if the light attenuation is high and generally will have a negligible effect on total photosynthetic rates of thicker communities.

As was stated in the Introduction, damage to photosystem II may occur without an apparent β. Such damage could lead to decreases in α. If some other factor, such as CO_2 limitation (Kromkamp et al. 1998), limits maximum photosynthetic rate, then it could be possible that photoinhibition effects explain some of our results. The steeper α (higher efficiency) with depth and lack of effect on P_{max} (Figs. 3, 6) may be indicative of such an effect, rather than photoacclimation.

A number of additional considerations should be addressed with respect to P-I relationships in periphyton communities. 1) Motile cells may move to habitats with optimal light. This decreases the probability of photoinhibition for these populations and will lead to a mat that is apparently saturated over a wide range of irradiance values (Kromkamp et al. 1998). The microelectrode measurements in our study were made too rapidly over fairly large distances using numerous increases and decreases in irradiance to be influenced much by this effect. Future models and experiments could address such measurements. 2) The variable light field associated with wave action and movement of periphyton masses in currents may lead to different responses than we observed. 3) We investigated periphyton collected from lotic systems; flow may alter photosynthetic rates (Dodds 1989b, Kühl et al. 1996). Lentic periphyton may be more prone to photoinhibition because of excessive O_2 concentrations (e.g. Carlton and Wetzel 1987) since O_2 is apparently involved in deactivation of photosystem II (Long et al. 1994). 4) Photosynthetic rate and repair of photoinhibition may vary significantly as a function of temperature and nutrients. Little is known about this for periphyton. 5) Microscale variation in mat architecture may be important in controlling microscale patterns of metabolism. In the future, methods may become available to assess *in situ* architecture of flocculant and filamentous periphyton communities.

Photosynthetic properties are functions of thickness of the periphyton. Taxonomic composition did not have a major influence when photosynthetic parameters of whole communities were assessed. However, taxonomic composition did appear to have an influence on light attenuation, which directly influenced the P-I parameters. It may be sufficient to model ecosystem productivity as a function of thickness of the periphyton mat with thickness scaled by light attenuation related to taxonomic composition. This would allow future models to link disturbances such as grazing and flooding to ecosystem production.

We are grateful for the technical assistance of Dolly Gudder, helpful discussions with Dr. Ian Hawes, and comments from anonymous reviewers. This research was supported by grants from the United States National Science Foundation, International Programs, to W.K.D. and R.L.L., and the New Zealand Foundation for Research Science and Technology Programmes ''Environmental Hydrology and Habitat Hydraulics'' (contract CO1519) and ''River Ecosystems'' (contract CO1210) to B.J.F.B. This is contribution 98-321-J from the Kansas Agricultural Experiment Station.

Anderson, J. M., Park, Y-I. & Chow, W. S. 1997. Photoinactivation and photoprotection of photosystem II in nature. *Physiol. Plant.* 100:214–23.

Biggs, B. J. F. 1987. The effects of sample storage and mechanical blending on the quantitative analysis of river periphyton. *Freshwater Biol.* 18:197–203.

Biggs, B. J. F. & Close, M. E. 1989. Periphyton biomass dynamics in gravel bed rivers: the relative effects of flows and nutrients. *Freshwater Biol.* 22:209–31.

Biggs, B. J. F. & Hickey, C. W. 1994. Periphyton responses to a hydraulic gradient in a regulated river, New Zealand. *Freshwater Biol.* 32:49–59.

Bothwell, M. L., Sherbot, D. M. J. & Pollock, C. M. 1994. Ecosystem response to solar ultraviolet-B radiation: influence of trophic-level interactions. *Science* 265:97–100.

Carlton, R. G. & Wetzel, R. G. 1987. Distributions and fates of oxygen in periphyton communities. *Can. J. Bot.* 65:1031–7.

Dodds, W. K. 1989a. Microscale vertical profiles of N_2 fixation, photosynthesis, O_2, chlorophyll *a*, and light in a cyanobacterial assemblage. *Appl. Environ. Microbiol.* 55:882–6.

——— 1989b. Photosynthesis of two morphologies of *Nostoc parmeloidies* (cyanobacteria) as related to flow velocities. *J. Phycol.* 25:199–209.

——— 1992. A modified fiber-optic light microprobe to measure spherically integrated photosynthetic photon flux density: characterization of periphyton photosynthesis-irradiance patterns. *Limnol. Oceanogr.* 37:871–8.

Enríquez, S. C., Duarte, M., Sand-Jensen, K. & Nielsen, S. L. 1996. Broad-scale comparison of photosynthetic rates across phototrophic organisms. *Oecologia* 108:197–206.

Glud, R. N., Ramsing, N. B. & Revsbech, N. P. 1992. Photosynthesis and photosynthesis-coupled respiration in natural biofilms measured by use of oxygen microsensors. *J. Phycol.* 28: 51–60.

Hill, W. 1996. Effects of light. *In* Stevenson, R. J., Bothwell, M. L. & Lowe, R. L. [Eds.] *Algal Ecology.* Academic Press, New York, pp. 121–48.

Hill, W. & Boston, H. L. 1991. Community development alters photosynthesis-irradiance relations in stream periphyton. *Limnol. Oceanogr.* 36:1375–89.

Jassby, A. D. & Platt, T. 1976. Mathematical formulation of the relationship between photosynthesis and light for phytoplankton. *Limnol. Oceanogr.* 21:540–7.

Jørgensen, B. B., Cohen, Y. & DesMarais, D. J. 1987. Photosynthetic action spectra and adaptation to spectral light distribution in a benthic cyanobacterial mat. *Appl. Environ. Microbiol.* 53:879–86.

Jørgensen, B. B. & DesMarais, D. J. 1988. Optical properties of benthic photosynthetic communities: fiber-optic studies of cyanobacterial mats. *Limnol. Oceanogr.* 35:1343–55.

Kromkamp, J., Barranguet, C. & Peene, J. 1998. Determination of microphytobenthos PSII quantum efficiency and photosynthetic activity by means of variable chlorophyll fluorescence. *Mar. Ecol. Prog. Ser.* 162:45–55.

Kühl, M., Glud, R. N., Ploug, H. & Ramsing, N. B. 1996. Microenvironmental control of photosynthesis and photosynthesis-

coupled respiration in an epilithic cyanobacterial biofilm. *J. Phycol.* 32:799–812.

Kühl, M., Lassen, C. & Revsbech, N. P. 1997. A simple light meter for measurements of PAR (400 to 700 nm) with fiber-optic microprobes: application for P vs E_0 (PAR) measurements in a microbial mat. *Aquat. Microbiol. Ecol.* 13:197–207.

LaBarbera M. & Vogel, S. 1976. An inexpensive thermistor flow meter for aquatic biology. *Limnol. Oceanogr.* 21:750–6.

Lassen, C., Ploug, H. & Jørgensen, B. B. 1992. A fibre-optic scalar irradiance microsensor: application for spectral light measurements in sediments. *FEMS Microbiol. Ecol.* 86:247–54.

Lassen, C., Revsbech, N. P. & Pedersen, O. 1997. Macrophyte development and resuspension regulate the photosynthesis and production of benthic microalgae. *Hydrobiologia* 350:1–11.

Long, S. P., Humphries, S. & Falkowski, P. G. 1994. Photoinhibition of photosynthesis in nature. *Ann. Rev. Plant Physiol. Plant Mol. Biol.* 45:633–62.

Lüning, K. 1979. Growth strategies of three *Laminaria* species (Phaeophyceae) inhabiting different depth zones in the sublittoral region of Helgoland (North Sea). *Mar. Ecol. Prog. Ser.* 1:195–207.

MacIntyre, H. L. & Cullen, J. J. 1995. Fine-scale vertical resolution of chlorophyll and photosynthetic parameters in shallow-water benthos. *Mar. Ecol. Prog. Ser.* 122:227–37.

Platt, T. C., Gallegos, L. & Harrison, W. G. 1980. Photoinhibition of photosynthesis in natural assemblages of marine phytoplankton. *J. Mar. Res.* 38:687–701.

Quinn, J. M., Cooper, A. B., Stroud, M. J. & Burrell, G. P. 1997. Shade effects on stream periphyton and invertebrates: an experiment in streamside channels. *New Zealand J. Mar. Freshwater Res.* 31:665–83.

Revsbech, N. P. & Jørgensen, B. B. 1983. Photosynthesis of benthic microflora measured by the oxygen microprofile method: capabilities and limitations of the method. *Limnol. Oceanogr.* 34:474–8.

Sand-Jensen, K. & Revsbech, N. P. 1987. Photosynthesis and light adaptation in epiphyte-macrophyte associations measured by oxygen microelectrodes. *Limnol. Oceanogr.* 32:452–7.

Sartory, D. P. & Grobbelaar, J. E. 1984. Extraction of chlorophyll *a* from freshwater phytoplankton for spectrophotometric analysis. *Hydrobiologia* 114:177–87.

Young, R. G. & Huryn, A. D. 1996. Interannual variation in discharge controls ecosystem metabolism along a grassland river continuum. *Can. J. Fish. Aquat. Sci.* 53:2199–211.